AIAA Atmospheric Flight Mechanics Conference
10 - 13 August 2009, Chicago, Illinois

AIAA 2009-6145

Adaptive Feedback Control Algorithm for Flutter Boundary Expansion

Jie Zeng*
ZONA Technology Inc, Scottsdale, Arizona, 85258, U.S.A

Raymond de Callafon†
University of California, San Diego, La Jolla, California, 92093, U.S.A

Martin Brenner‡
NASA Dryden Flight Research Center, Edwards, California, 93523, U.S.A

This paper introduces an adaptive flutter suppression control algorithm which is based on the iterative estimate of the aeroelastic plant and design of the feedback controller. In this algorithm, the dual-Youla parametrization is implemented as an essential part to estimate the open loop aeroelastic model from the closed loop experiment. The advantage of utilizing the dual-Youla parametrization for the aeroelastic plant estimation is that the possible unstable open loop aeroelastic model could be estimated in the situation where aeroelastic dynamic system is operating above the flutter speed. Based on the estimated open loop model, a new controller could be designed using the standard controller design techniques to extend the flutter envelope boundary. By iteratively estimating the open loop aeroelastic model and designing the controller, the flutter boundary could be expanded. Application of this adaptive control algorithm to the pitch-plunge aeroelastic system shows that the flutter boundary can be expanded by 80%.

Nomenclature

$G(q)$	Aeroelastic Plant
$K(q)$	Feedback Control
(N, D)	Right Coprime Factor of $G(q)$
(N_k, D_k)	Right Coprime Factor of $K(q)$
$T(G, K)$	Feedback Connection between $G(q)$ and $K(q)$
U	Air Speed, m/s
f	Frequency, Hz
h	Plunge
α	Pitch
β	Flap
ξ	Damping Ratio
Subscript	
i	Iteration number

*R & D Control System Engineer, Member AIAA. jzeng@zonatech.com
†Associate Professor. calafon@ucsd.edu
‡Aerospace Engineer, Member AIAA. Martin.J.Brenner@nasa.gov

I. Introduction

Flutter control becomes increasingly important as the aircraft design moves towards lighter weight material to improve the fuel efficiency and aircraft agility. Extensive research on active flutter suppression has been conducted during the last decade, and various control methodologies has been employed to develop the flutter control schemes.[1–11] All of these methods provide promising results for flutter suppression.

In order to design an optimal controller for flutter suppression, a sufficient mathematical aeroelastic model, which is computed with the use of finite element method, a panel aerodynamic method, and the minimum state space realization of the equation of motion, is commonly adopted. However, because the aeroelastic system changes significantly with different flight conditions, the fixed controller may only stabilize the aeroelastic system in a small range of the flight conditions. Therefore, different controllers are required to cover the entire flight envelope. The gain-scheduled controller is an option for active flutter suppression.[10] However, these gain-scheduled controllers whose design is based on the analytical aeroelastic model, may not accommodate the real dynamics of the aeroelastic system. An alternative solution to overcome this drawback is to design the feedback controller from the aeroelastic model which is estimated on-line consistently using flight test data. By iteratively estimating the aeroelastic model and designing the model based controller, the closed loop aeroelastic system could be more robust, and the flutter boundary maybe be largely expanded compared to the fixed control method[11] or gain-scheduled control method.[10]

Apparently, the aeroelastic system is open loop unstable above its flutter speed. To facilitate the estimate of a unstable open loop system, a stabilized closed loop experiment must be performed to obtain a desired input/output experiment data. Furthermore, for a direct estimation of an open loop unstable aeroelastic model, a dual-Youla parametrization methodology will be applied in this paper. Impressive results are obtained to illustrate the application of the proposed adaptive control algorithm to the pitch-plunge aeroelastic system.

II. Open Loop Aeroelastic Model Identification Using Dual-Youla Parametrization

Assuming the feedback connection $T(G,K)$, is internally stable (Figure 1), and the open loop aeroelastic plant, G, has a Right Coprime Factorization (rcf), $G = ND^{-1}$, and a stable controller, K, also has a right coprime factorization with $K = N_k D_k^{-1}$, then there exists a $R_0 \in RH_\infty$ that characterizes the (N, D) of the plant G as

$$\begin{aligned} N &= N_0 + D_k R_0 \\ D &= D_0 - N_k R_0 \end{aligned} \tag{1}$$

where (N_0, D_0) is a rcf of any auxiliary plant that satisfying $T(G_0, K) \in RH_\infty$. R_0 is an unknown stable transfer function. Therefore, the estimation of the unknown stable transfer function, R_0, will yield an estimate $(\hat{N}, \hat{D})$ of the open loop aeroelastic plant $\hat{G}$.

$$\begin{aligned} \hat{N} &= N_0 + D_k \hat{R}_0 \\ \hat{D} &= D_0 - N_k \hat{R}_0 \end{aligned} \tag{2}$$

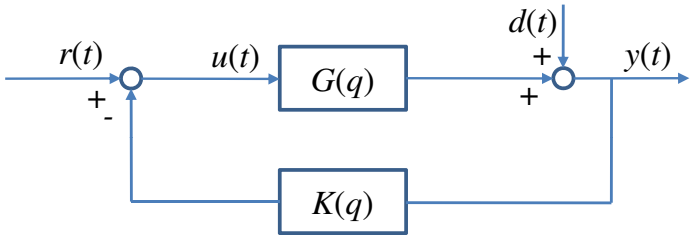

Figure 1. Feedback Control System.

Using a rcf pair (N_0, D_0) of plant G, a rcf pair (N_k, D_k) of the controller K and the stable transfer function R_0, the representation of the feedback connection $T(G,K)$ in terms of the dual-Youla parametrization has been depicted in Figure 2.

In Figure 2, the intermediate signals, $x(t)$ and $z(t)$, are related by the transfer functions R_0 and S_0.

$$z(t) = R_0 x(t) + S_0 d(t)$$

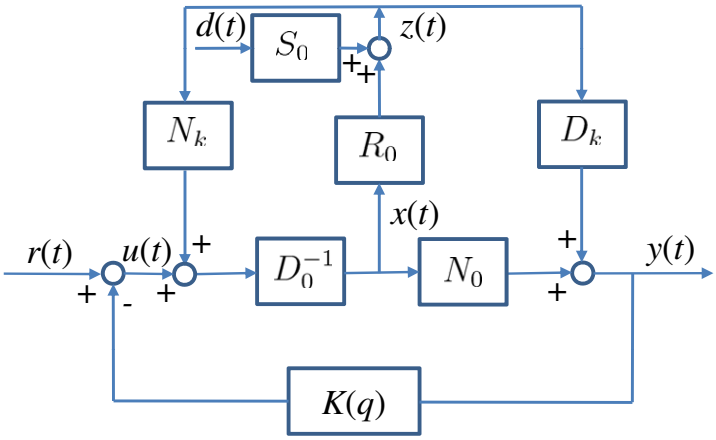

Figure 2. Reformulation of the Feedback Control System.

where $d(t)$ is external disturbance.

If $x(t)$ and $z(t)$ are known, then R_0 and/or S_0 can be estimated by standard system identification techniques.[12] From a simple mathematical derivation, the intermediate signal $x(t)$ can be defined as

$$x(t) = (D_0 + KN_0)^{-1} \begin{bmatrix} K & I \end{bmatrix} \begin{bmatrix} y \\ u \end{bmatrix} \tag{3}$$

and signal $z(t)$ is defined as

$$z(t) = (D_k + G_0N_k)^{-1} \begin{bmatrix} I & G_0 \end{bmatrix} \begin{bmatrix} y \\ u \end{bmatrix} \tag{4}$$

It should be noted that R_0 can also be estimated with the use of the on-line system identification technique, such as the recursive least square (RLS) adaptive filtering algorithm. In this case, a Finite Impulse Response (FIR) filter, or Orthonormal FIR filter structure can be applied to approximate R_0. For details of the on-line modeling of R_0, please refer to.[13]

III. Controller Design

With the computed aeroelastic model $\hat{G}$ from Eq. (2) in place, a new feedback controller, $K(q)$, can be designed using any standard control techniques from simple classic control technique such as Proportional Integral Derivative(PID) control to modern/robust control technique such as Linear Quadratic Gaussian (LQG) control, H_2 control, H_∞ control , or μ synthesis technique.[14] In this paper, only a simple proportional controller, $K(q)$, is applied to the pitch-plunge system for flutter suppression.

IV. Summary of the Adaptive Control Algorithm

The procedure to iteratively estimate a stable/unstable aeroelastic system with a closed loop experiment and design the controller is described as follows:

- A feedback controller is designed to stabilize the aeroelastic system at low airspeed, and furthermore, it can cover a small range of airspeed locations over the open loop flutter speed.
- Find a stable nominal open loop aeroelastic model below the flutter speed as a reference model.
- Identify the open loop unstable aeroelastic model using dual-Youla method.
- Design the new controller using the new aeroelastic model.

The iteration stops when it is difficult to find a new controller to stabilize the open loop aeroelastic system.

V. Application to the Pitch-Plunge Aeroelastic System

The process of iteratively estimating the aeroelastic system and designing of the control is applied to a pitch-plunge system. This system is comprised of a rigid airfoil, whose motion is restricted to pitching and plunging, mounted in a wind tunnel at Texas A & M University.[15]

The prototypical pitch-plunge aeroelastic system is shown in Figure 3.

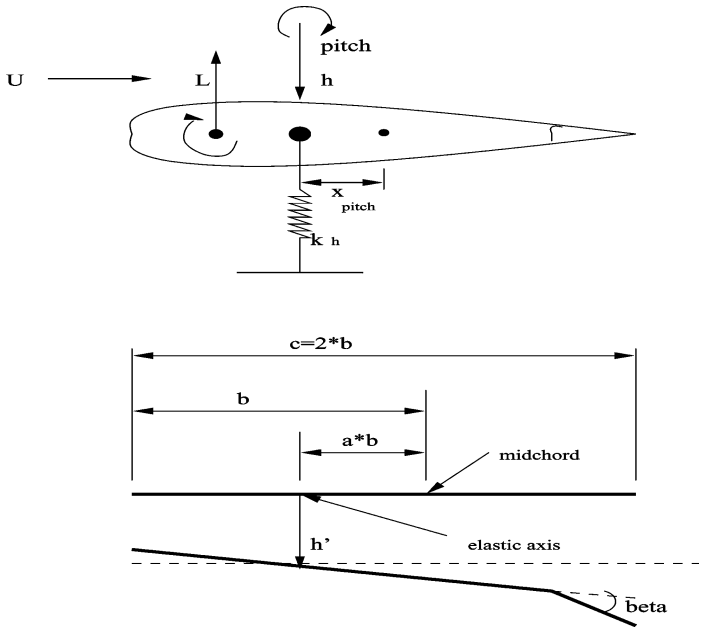

Figure 3. Pitch-Plunge Aeroelastic System.

The dynamics of the pitch-plunge aeroelastic system are described to within a high-degree of accuracy by Eq. (5),

$$\begin{bmatrix} m_T & m_w x_\alpha b \\ m_w x_\alpha b & I_\alpha \end{bmatrix} \begin{bmatrix} \ddot{h} \\ \ddot{\alpha} \end{bmatrix} + \begin{bmatrix} c_h & 0 \\ 0 & c_\alpha \end{bmatrix} \begin{bmatrix} \dot{h} \\ \dot{\alpha} \end{bmatrix} + \begin{bmatrix} k_h & 0 \\ 0 & k_\alpha \end{bmatrix} \begin{bmatrix} h \\ \alpha \end{bmatrix} = \bar{q} 2b \begin{bmatrix} c_{l_\alpha} \left(\alpha + \frac{1}{U}\dot{h} + \left(\frac{1}{2} - a\right) b \frac{1}{U}\dot{\alpha} \right) + c_{l_\beta}\beta \\ c_{m_\alpha} \left(\alpha + \frac{1}{U}\dot{h} + \left(\frac{1}{2} - a\right) \frac{b}{U}\dot{\alpha} \right) + c_{m_\beta}\beta \end{bmatrix} \tag{5}$$

These dynamics describe the complete aeroelastic system. The degrees of freedom of the rigid airfoil are described by the plunge, h, and the pitch, α, parameters. The left side of the equality describes the quasi-steady aerodynamics that are generated in response to motion of the airfoil and commanded rotations, β, of a flap. The right side of the equality describes the structural dynamics. The parameters describing the dynamics of the system are given in Table 1. These parameters are generally indicative of those presented in several references.

Table 1. Pitch-Plunge System Parameters.

parameter		parameter	
a	= -0.6	k_α	= 2.82
b	= 0.135 *m*	ρ	= 1.225 kg/m^3
m	= 12.387 *kg*	x_α	= 0.2466
I_α	= 0.065 $m^2 kg$	k_h	= 2844.4 *N/m*
c_α	= 0.180 $m^2 kg/s$	c_h	= 27.43 *kg/s*
c_{l_α}	= 6.28	c_{m_α}	= -0.628
c_{l_β}	= 3.358	c_{m_β}	= -0.635

The simulink block of this pitch-plunge aeroelastic system is illustrated in Figure 4.

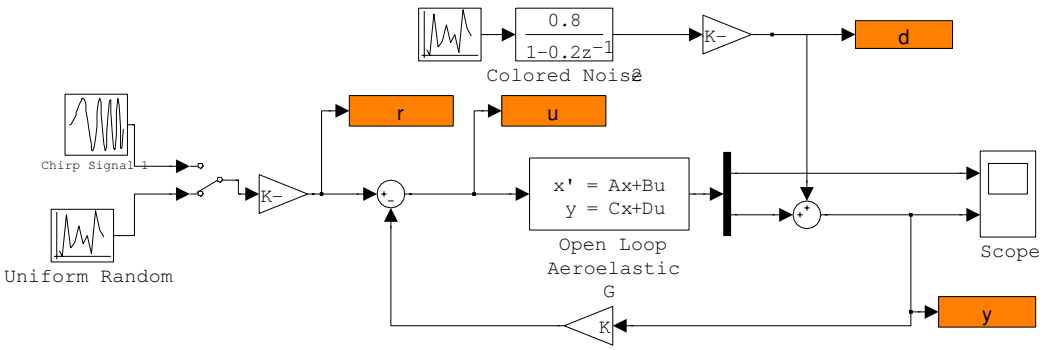

Figure 4. The Close Loop Pitch-Plunge Aeroelastic Simulink Model.

The open loop flutter can be found easily by perturbing the airspeed, U, until the aeroelastic system becomes unstable. The calculation results of the modes of the open loop aeroelastic system is shown in Table 2.

Table 2. Open Loop Flutter Speed.

$U\ [m/s]$	10	11	12	12.1	12.5
Frequency f [Hz]	1.4699	1.6061	1.7638	1.789	1.8212
	2.3696	2.243	2.1142	2.0989	2.0835
Damping ξ	0.2210	0.2400	0.2951	0.3102	0.3326
	0.0877	0.0609	0.0086	-0.0074	-0.0314

From Table 2, it is seen that the open loop system becomes unstable above the air speed of $U = 12.1\ m/s$. A simple negative feedback proportional control, K, is designed using a stable open loop aeroelastic system at the air speed of $U = 11\ m/s$. with $K_1 = 0.2727$, the flutter speed can be extended to $13.3\ m/s$. The flutter speed result is illustrated in Table 3.

Table 3. Close Loop Flutter Speed with $K_1 = 0.2727$.

$U\ [m/s]$	10	11	12	12.5	13	13.3
Frequency f [Hz]	1.3572	1.4484	1.5657	1.6349	1.7033	1.7391
	2.4461	2.355	2.2405	2.1766	2.1197	2.0943
Damping ξ	0.2283	0.2312	0.2496	0.2678	0.2951	0.3147
	0.0942	0.0853	0.0659	0.0471	0.01841	-0.0023

Because the open loop aeroelastic system is unstable above the airspeed $12\ m/s$, and the closed loop aeroelastic system is unstable above the airspeed $13\ m/s$ with the controller K_1, it can not be directly estimated using the input signal, u, and output signal, y, or use indirect closed loop identification method. A dual-Youla identification method described in the above section is applied to estimate the unstable open loop aeroelastic system, G. A closed loop experiment is performed at the airspeed of $U = 13\ m/s$. From Eq. (1), a nominal model, G_0, with rcf pair (N_0, D_0) is required, and in this case, a stable open loop aeroelastic model at airspeed $U = 10\ m/s$ is selected as the reference model. Collecting the signals, r, u, and y, from the simulink process, the intermediate signals $x(t)$ and $z(t)$ can be constructed. A simple 4th order output error model $\hat{R}$ of R_0 is estimated. Finally, the unstable open loop aeroelastic model, G, with a rcf pair $(\hat{N}, \hat{D})$ can be computed via

$$\begin{aligned} \hat{N} &= N_0 + D_k\hat{R} \\ \hat{D} &= D_0 - N_k\hat{R} \end{aligned} \tag{6}$$

A comparison between the estimated unstable open loop aeroelastic model and the true aeroelastic system at $U = 13\ m/s$ is shown in Figure 5.

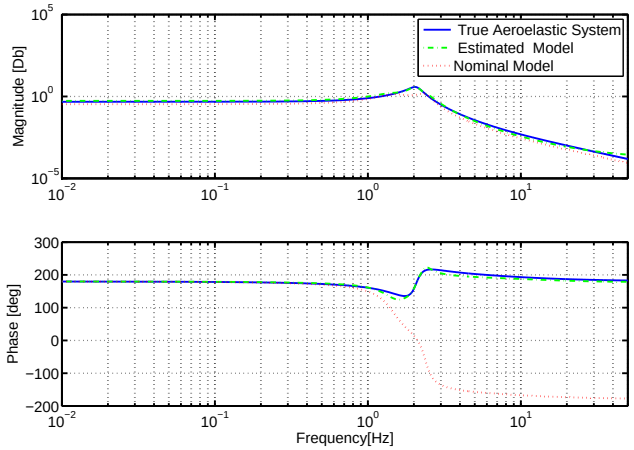

Figure 5. Comparison of the True Unstable System and Estimated Unstable Model at $U = 13\ m/s$ and $K_1 = 0.2727$.

From Figure 5 it is obtained that the estimated unstable model can fit the true unstable aeroelastic system very well. With this estimated aeroelastic model, a new controller can be designed, and is computed as $K_2 = 0.5455$. With this new designed controller, K_2, the closed loop flutter speed can be extended to $U = 15\ m/s$. The flutter speed result is shown in Table 4.

Table 4. Close Loop Flutter Speed with $K_2 = 0.5455$.

$U\ [m/s]$	10	11	12	12.5	13	14	15
Frequency f [Hz]	1.2533	1.3115	1.3824	1.4239	1.4703	1.5781	1.6844
	2.5118	2.4458	2.3668	2.3215	2.2717	2.1623	2.071
Damping ξ	0.2286	0.2340	0.2423	0.2483	0.2564	0.2846	0.3355
	0.0980	0.0935	0.0861	0.0804	0.0725	0.0442	-0.0084

The unstable open loop aeroelastic model is estimated again using the dual-Youla identification method at the operation conditions of $U = 14\ m/s$ and $K_2 = 0.5455$, the estimation results are shown in Figure 6.

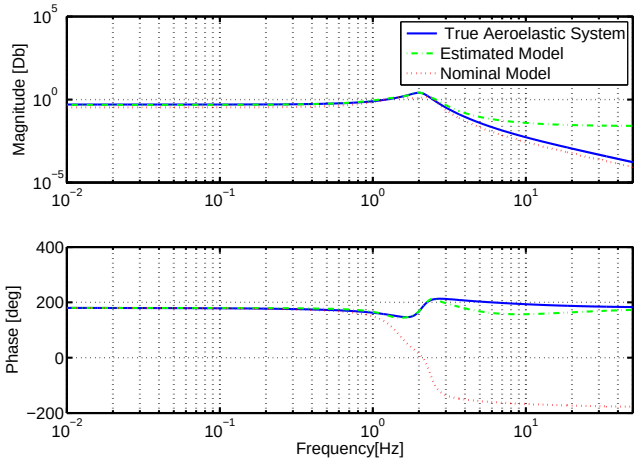

Figure 6. Comparison of the True Unstable System and Estimated Unstable Model at $U = 14\ m/s$ and $K_2 = 0.5455$.

With the new estimated open loop aeroelastic model, a new controller, $K_3 = 0.82885$, can be designed to extend

the flutter speed to $U = 17.5\ m/s$. The result of the flutter speed is illustrated in Table 5.

Table 5. Close Loop Flutter Speed with $K_3 = 0.82885$.

$U\ [m/s]$	12	13	14	15	16	17	17.5
Frequency f [Hz]	1.2169	1.2593	1.3098	1.3705	1.4427	1.5217	1.5588
	2.4711	2.4094	2.3385	2.2573	2.1669	2.0770	2.0389
Damping ξ	0.2499	0.2578	0.2681	0.2826	0.3048	0.3398	0.3624
	0.0949	0.0901	0.0828	0.0711	0.0512	0.0176	-0.0047

Keep iteratively estimating the unstable open loop aeroelastic model, and using this model to design a new controller, the flutter speed can be further extended towards $U = 23\ m/s$, which is almost double the open loop flutter $U = 12.1\ m/s$. Figure 7 is the comparison of the estimated open loop aeroelastic model and the true aeroelastic model at $U = 17\ m/s$ and $K_3 = 0.82885$. Figure 8 is the comparison of the estimated open loop aeroelastic model and the true aeroelastic model at $U = 19.5\ m/s$ and $K_4 = 0.9905$. Table 6 is the closed loop flutter speed computed with the controller, $K_4 = 0.9905$. Table 7 is the closed loop flutter speed computed with the controller $K_5 = 1.1125$. The final results of the flutter speed with different K are illustrated in Figure 9(a) and Figure 9(b).

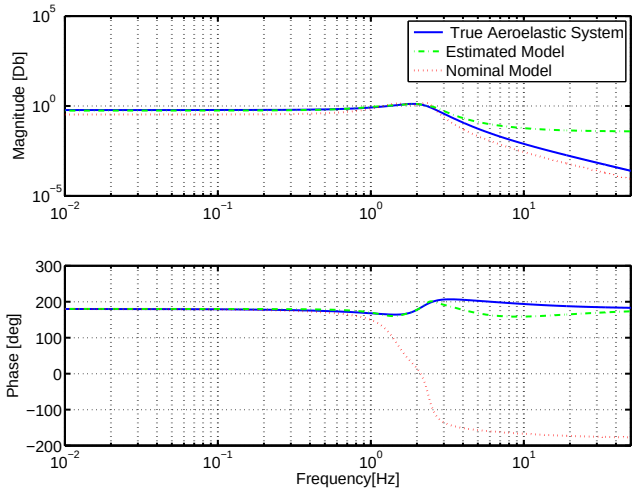

Figure 7. Comparison of the True Unstable System and Estimated Unstable Model at $U = 17\ m/s$ and $K_3 = 0.82885$.

Table 6. Close Loop Flutter Speed with $K_4 = 0.9905$.

$U\ [m/s]$	16	17	17.5	18	19	19.5	20
Frequency f [Hz]	1.2406	1.2818	1.3048	1.3294	1.3815	1.4074	1.4320
	2.2925	2.2184	2.1791	2.1387	2.0578	2.0197	1.9849
Damping ξ	0.2999	0.3166	0.3269	0.3389	0.3690	0.3874	0.4078
	0.0779	0.0666	0.0590	0.0497	0.0243	0.0079	-0.0107

Table 7. Close Loop Flutter Speed with $K_5 = 1.1125$.

$U\ [m/s]$	18.0	19.0	19.5	20	21	22	23
Frequency f [Hz]	1.1288	1.1461	1.1555	1.1653	1.1856	1.2055	1.2229
	2.2540	2.1878	2.1532	2.1179	2.0461	1.9748	1.9075
Damping ξ	0.3432	0.3633	0.3747	0.3872	0.4159	0.4500	0.4895
	0.0751	0.0655	0.0595	0.0526	0.0355	0.0133	-0.0141

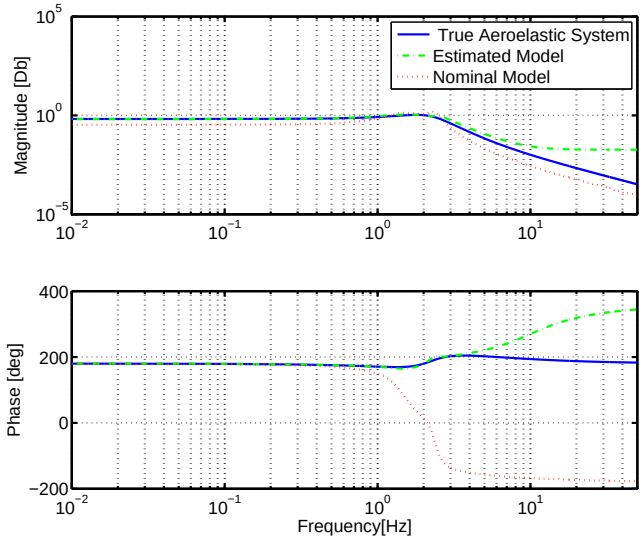

Figure 8. Comparison of the True Unstable System and Estimated Unstable Model at $U = 19.5\ m/s$ and $K_4 = 0.9905$.

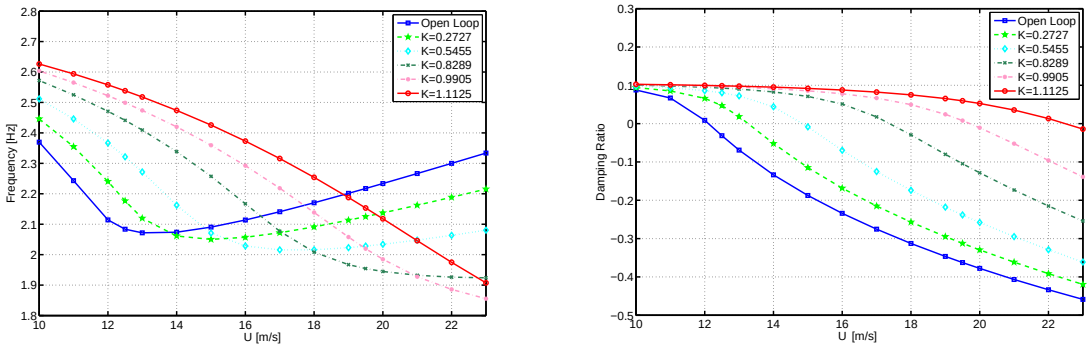

(a) Frequency

(b) Damping Ratio

Figure 9. Frequency/Damping Varying of the Critical Mode as a Function of Air Speed U.

From Figure 9(a) and Figure 9(b) it is demonstrated that with the proposed adaptive control method, the flutter speed of the pitch-plunge aeroelastic system can be largely extended.

VI. Conclusions

In this paper, an adaptive feedback control algorithm based on the iteratively estimate of the aeroelastic plant and design of the feedback controller is introduced. The advantage of this adaptive algorithm lies in the fact that firstly the open loop unstable aeroelastic model can be directly estimated with the use of the dual-Youla parametrization; secondly a new model-based controller can be easily designed using the standard control techniques. As a result, a better performance of the controller for flutter suppression can be obtained. Application of this adaptive control algorithm to the pitch-plunge aeroelastic system shows that the flutter boundary is largely expanded.

Acknowledgments

This research is supported by NASA Dryden Flight Research Center under a Small Business Innovation Research (SBIR) Phase I program.

References

[1]Newsom, J. R., "Control Law Synthesis for Active Flutter Suppresion Using Optimal Control Theory," *Journal of Guidance, Control, and Dynamics*, Vol. 2, No. 5, 1979, pp. 388–394.

[2]Horikawa, H. and Dowell, E., "An Elementary Explanation of the Flutter Mechanism with Active Feedback Controls," *Journal of Aircraft*, Vol. 16, No. 4, 1979, pp. 225–232.

[3]Mahesh, J. K., Stone, C. R., Garrard, W. L., and Dunn, H. J., "Control law synthesis for flutter suppression using linear quadratic control theory," *Journal of Guidance, Control, and Dynamics*, Vol. 4, No. 4, 1981, pp. 415–422.

[4]Garrard, W. L. and Liebst, B. S., "Active Flutter Suppression using eigenspace and linear quadratic design techniques," *Journal of Guidance, Control, and Dynamics*, Vol. 8, No. 3, 1985, pp. 304–311.

[5]Schmidt, D. and Chen, T., "Frequency domain synthesis of a robust flutter suppression control law," *Journal of Guidance, Control, and Dynamics*, Vol. 9, No. 3, 1986, pp. 346–351.

[6]Leibst, B. S., Garrard, W. L., and Farm, J. A., "Design of a Multivariable Fluter Suppression/Gust Load Alleviation System," *Journal of Guidance, Control, and Dynamics*, Vol. 11, No. 3, 1988, pp. 220–229.

[7]Waszak, M. R. and Srinathkumar, S., "Flutter Suppression for the Active Flexible Wing," *Journal of Aircraft*, Vol. 32, No. 1, 1995, pp. 61–67.

[8]Eversman, W. and Roy, I. D., "Active flutter suppresion using MIMO adaptive LMS control," *37th AIAA/ASME/ASCE/AHS/ASC Structures, Structural Dynamics, and Material Conference and Exhibit*, Salt Lake, UT, 1996, AIAA-1996-1345.

[9]Andrighettoni, M. and Mantegazza, P., "Multi-input/multi-output adaptive active flutter suppression for a wing model," *Journal of Aircraft*, Vol. 35, No. 3, 1998, pp. 462–469.

[10]Barker, J. M., Balas, G. J., and Blue, P. A., "Active flutter suppression via gain-scheduled linear fractional control," *Proceedings of the American Control Conference*, San Diego, California, 1999, pp. 4014–4018.

[11]Han, J. H., Tani, J., and Qiu, J. H., "Active Flutter Suppression of a Lifting Surface Using Piezoelectric Actuation and Model Control Theory," *Journal of Sound and Vibration*, Vol. 291, 2006, pp. 706–722.

[12]Ljung, L., *System Identification: Theory for the User*, Prentice-Hall, Englewood Cliffs, NJ, 1999.

[13]Zeng, J. and de Callafon, R. A., "Recursive Filter Estimation for Feedforward Noise Cancellation with Acoustic Coupling," *Journal of Sound and Vibration*, Vol. 291, 2006, pp. 1061–1079.

[14]Skogestad, S. and Postlethwaite, I., *Multivariable Feedbacl Control: Analysis and Design*, John Wiley and Sons, Ltd, West Sussex, England, 2005.

[15]Ko, J., Kurdila, A. J., and Strganac, T. W., "Nonlinear Control of a Prototypical Wing Section with Torsional Nonlinearity," *Journal of Guidance, Control, and Dynamics*, Vol. 20, No. 6, Nov.-Dec. 1997, pp. 1181–1189.